The Geography of Partisan Homophily in the 2020 US Presidential Election

Abstract

Partisan segregation in the United States is often interpreted as evidence of limited social interaction among out-partisans, or partisan homophily. In this paper, I draw on 2020 US presidential election results and data on the pairwise density of social ties between the populations of 22,537 zip code tabulation areas (ZCTA) to examine how different areas are socially connected to politically similar others. Using the local Moran index, I first identify clusters of ZCTAs where there is evidence of partisan homophily or heterophily. In a series of multinomial logistic regressions, I then also examine differences in the probability of each cluster across different settlement types and regions, and across areas with differences in the relative connectedness and geographic distance to others. I find that partisan homophily is the norm across areas, broadly tracking partisan segregation along the urban-rural continuum. However, the populations of Democratic-leaning areas, which are most likely to be in cities and suburbs, are on average likely to have more of their co-partisan social ties in relatively distant areas when compared to the populations of Republican-leaning areas. This highlights the prospect of partisan differences in the role of non-local context in local political outcomes.

Keywords: Partisan Homophily; Partisan Segregation; US Presidential Elections

1 Introduction

Residential segregation by partisanship, or partisan segregation, has been on the rise in the United States over the last few decades. Between the 1992 and 2020 presidential elections, the share of the electorate that lived in counties where the winning candidate gained more than 60 per cent of the two-party vote—often termed 'landslide' counties—gradually rose from roughly 30 per cent to 58 per cent (Bishop, 2020; Darmofal and Strickler, 2019).[1] While such trends are not unprecedented in American electoral history, the recent rise in partisan segregation is characterised by a distinctive urban-rural divide (Mettler and Brown, 2022): Democratic candidates have been gaining higher shares of the vote in more urbanised areas, with Republicans largely dominating elsewhere. Importantly, partisan segregation is also observed at fine spatial resolutions (e.g. Brown and Enos, 2021; Johnston et al., 2020; Kinsella et al., 2021, 2015; Myers, 2013; Rohla et al., 2018; Scala and Johnson, 2017); indeed, even within Democratic-leaning metropolitan counties, the electoral scale has been shown to tip in favour of Republican candidates as one moves away from metropolitan cores.

The relative importance of different factors in the recent rise of partisan segregation has been a subject of lively scholarly and public debate. The residential sorting thesis, which was popularised by Bishop and Cushing (2009), posits that Americans have been more likely to move to areas that are populated by co-partisans, either due to being drawn to like-minded others or socio-cultural factors that correlate with partisanship. However, more systematic work has shown that while partisanship and its correlates do factor into mobility decisions, they are usually outweighed by more universal criteria such as housing affordability, school quality, and the prevalence of crime (Gimpel and Hui, 2015; Martin and Webster, 2020; Mummolo and Nall, 2017). As these factors are expected to constrain mass sorting into politically homogeneous areas, attention has shifted to alternative explanations, such as partisan conversion—be it due to changing local, structural, or institutional conditions—and the replacement of older voters with the young and new. Indeed, using registration data on the near-universe of American voters, Brown et al. (2023) identify generational change and switches in party affiliation as the leading drivers of changes in county-level partisan homogeneity between 2008 and 2020 in Democratic-leaning and Republican-leaning areas respectively.[2]

[1] A steeper trend emerges in the share of counties that saw a landslide victory, which rose from roughly 26 to 77 per cent between 1992 and 2020 (Bishop, 2020; Darmofal and Strickler, 2019).

[2] For changes in partisan homogeneity in Democratic-leaning counties, Brown et al. (2023) also identify new adult entries in the electorate, which include immigrants, as an important driver. In line with the residential sorting thesis, the authors also find that mobility plays a role in counties of both leanings, albeit at a much lesser extent than other drivers.

Many have called attention to the potential implications of rising partisan segregation. One concern is that the concentration of Democratic voters in densely populated, single-seat districts can magnify the disconnect between the popular vote and the partisan composition of local, state, and national legislatures (Chen and Rodden, 2013; Hopkins, 2017; Rodden, 2019). This can then also give rise to discrepancies between implemented policies and policy preferences; for instance, Nall (2018) argues that partisan segregation within metropolitan areas led to the neglect of urban preferences for public transit in favour of suburban preferences for new roads. Finally, others fear that segregation promotes polarisation (e.g. Bishop and Cushing, 2009; Enos, 2017): to the extent that voters interact with others in their residential environment, the spatial clustering of co-partisans may restrict exposure to others with differing political identities and views. As experimental evidence suggests that intergroup contact often acts to constrain affective and ideological distance between disparate social groups (Mutz, 2002; Pettigrew and Tropp, 2006), this may have plausibly contributed to the rise in inter-partisan animosity (Finkel et al., 2020; Iyengar et al., 2019) and intra-partisan ideological homogeneity (Boxell et al., 2017; Gentzkow, 2016) recorded in recent decades, with adverse implications for the function of democratic institutions.[3,4]

The link between rising partisan segregation and issues around political representation is straightforward: as with the related issue of partisan gerrymandering (McGhee, 2020), these merely arise from changes in the arrangement of partisans across political boundaries. Though the claim that partisan segregation implies limited intergroup contact, which might in turn be contributing to political polarisation, is arguably more controversial. As Abrams and Fiorina (2012) suggest, this crucially rests on the assumption that, by and large, an American voter's residential environment—at whatever spatial scale this might be measured—is indeed a sound proxy for their social network. Questions of this sort have interested electoral geographers and urban sociologists for some time. Albeit often constrained by data limitations, relevant work has consistently shown that the spatial concentration of Americans' social ties can vary substantially depending on the kind of settlement in which they reside as well as their demographic characteristics, with higher earners residing in more urbanised areas being more likely to have more geographically distant social ties (e.g. Baybeck and Huckfeldt, 2002a,b; Fischer, 1982; Huckfeldt, 1983, 1982; Logan and Spitze, 1994).

[3]With respect to ideological polarisation, Gentzkow (2016) demonstrates that Americans generally do not hold more extreme views than they used to, but partisans are more likely to hold opposing viewpoints than in the past.

[4]As shown by Mason (2015) and others, inter-partisan animosity does not presuppose ideological distance between partisans. Moreover, partisan affect has been shown to act as a strong cue for non-political judgements and behaviours among Americans (Iyengar and Westwood, 2015).

Also emphasised in this literature is the role of telephony and the Internet in expanding the geographic distance over which Americans interact with kin and non-kin alike (e.g. Mok et al., 2007, 2010; Takhteyev et al., 2012; Wellman, 1979, 1996; Wellman and Potter, 1999; Wellman et al., 2003). Indeed, using data on social media friendships, Bailey et al. (2018) find that, on average, the share of social ties of a county's population living more than 200 miles away is 30 per cent. These findings suggest that while partisan segregation may be indirectly informative about partisan homophily—the tendency of voters in any given area to be more socially connected to those who voted similarly elsewhere—it may conceal its true extent or the geographic ranges over which it occurs.[5]

In this paper, I explore partisan homophily across zip code tabulation areas (ZCTA) in the United States using data on voting behaviour in the 2020 presidential election and on the density of Facebook friendships between ZCTA-pairs shortly after the election. I operationalise partisan homophily as autocorrelation of voting behaviour in social space using the local Moran index, which allows me to identify clusters of ZCTAs of different partisan leanings where there is strong evidence of partisan homophily or heterophily with respect to social ties in other areas. With ZCTAs as the level of measurement, partisan homophily (heterophily) describes cases where the population of a given area tends to have denser social ties with those of others with a similar (dissimilar) composition of partisan vote shares. I find that 70 per cent of the US population resides in relatively homophilous areas, with a further 7 and 23 per cent respectively residing in relatively heterophilous areas and areas where there is insufficient evidence of homophily or heterophily.

Employing multinomial logistic regressions, I also examine the probability of membership in each local Moran cluster for areas in different regions and settlement types. I show that Democratic-leaning cities and suburbs are more likely to be both homophilous and heterophilous when compared to rural, Republican-leaning areas, while cities and suburbs of the South are the most likely to be heterophilous. In additional specifications, I also examine the probability of cluster membership for areas with differences in the relative density and geographic distance of social ties in other areas. Overall, the findings suggest that while partisan homophily broadly tracks partisan segregation along the urban-rural continuum, voters in Democratic-leaning areas are more likely to interact with relatively distant co-partisans than those in Republican-leaning areas. On average, homophilous areas that are in the fifth quintile in terms of the relative connectedness and distance to their social ties in other areas are respectively 37 and 6.4 times more likely to be Democratic-leaning rather than Republican-leaning.

[5]As defined by McPherson et al. (2001), homophily is 'the principle that a contact between similar people occurs at a higher rate than among dissimilar people'.

The empirical contribution of this paper is threefold. First, it offers the first country-wide ecological study of partisan homophily in the United States using data on the social ties rather than the geographic distances between the populations of disparate areas. This addresses a long-standing quagmire in relevant literature whereby the observation of partisan residential segregation is typically equated with that of partisan homophily. As such, the focus of this paper on actual social ties allows for a more accurate and nuanced assessment of the extent in which different areas in the United States are politically homophilous. Second, this paper also contributes to a growing literature examining the electoral geography of the United States at fine spatial resolutions. Namely, it complements a small number of studies of voting patterns at the below-county level (e.g. Johnston et al., 2020; Kinsella et al., 2021, 2015; Myers, 2013; Rohla et al., 2018), offering a deeper understanding of local political context in different types of settlement along the urban-rural continuum. Lastly, this paper is linked to conceptual work on the uncertain geographic context problem in spatial analysis (Kwan, 2012; Fowler et al., 2020), elucidating its implications for the geographic study of electoral outcomes in the United States. That is, given that social interactions with co-partisans are an important contextual influence on political preferences (Huckfeldt and Sprague, 1995), the findings highlight differences in the geographic distances over which this is likely to be exerted on voters in different kinds of localities.

2 Data and Methods

2.1 Social Connectedness Index

I observe the relative density of social ties between ZCTAs across the United States using the Social Connectedness Index (SCI) by Bailey et al. (2020).[6] This is based on all active users of Facebook—the popular online social networking service—as of October 2021, and is computed for ZCTA-pairs ij as follows:[7]

$$SCI_{ij} = SCI_{ji} = \phi \frac{FB\_Friendships_{ij}}{FB\_Users_i \times FB\_Users_j} \tag{1}$$

The SCI is thus the total number of Facebook friendships between users in i and j over the product of users in each area, scaled by a factor ϕ. The latter is applied for privacy purposes and ensures that the index will range from 1 to

[6]The SCI is publicly available and distributed via the Humanitarian Data Exchange of the United Nations Office for the Coordination of Humanitarian Affairs.

[7]A Facebook user is deemed active when they have used the service in the previous 30 days.

1,000,000. Consequently, when comparing any two ZCTA-pairs, higher values of the index denote a higher density of Facebook friendships by a factor that is equal to the ratio of the higher value over the lower value.[8] Note that the SCI is available for for 22,537 out of the total 33,642 ZCTAs spanning the United States as it is suppressed for areas where there are very few users. These areas are thus necessarily excluded from the analysis in this paper. As shown on Appendix Figure A.1, these are mainly concentrated in sparsely populated regions of the Midwest and the West, and account for under 2 per cent of the total population.

As discussed by Bailey et al. (2020), there is growing evidence that Facebook friendships closely resemble real-world social ties among Americans. Indeed, surveys suggest that almost 70 per cent of adults in the United States were Facebook users as of 2021 (Vogels and Anderson, 2021) and that the vast majority of users who are friends on Facebook have met in-person (Duggan et al., 2015). What is more, there is evidence to suggest that there is little variation in Facebook usage rates by partisanship, settlement type, and demographic characteristics (Vogels and Anderson, 2021; Vogels et al., 2021). The SCI is thus plausibly a sound proxy for the density of social ties between localities. This is further corroborated in recent empirical studies that use the SCI to identify spatial spillover effects in diverse domains ranging from public health (Charoenwong et al., 2020; Holtz et al., 2020; Kuchler et al., 2022; Zhao et al., 2021) to consumer behaviour (Makridis, 2022) and finance (Wilson, 2022). For instance, looking at the spread of disease during the COVID-19 pandemic, Kuchler et al. (2022) find that a county's social proximity to COVID-19 'hotspots' as measured by the SCI were predictive of the geographic spread of the disease even when controlling for geographic distance.

In expressing the neighbourhood relations between ZCTA-pairs, I first construct a social neighbour matrix $\mathbf{A}$ with elements a_{ij} as follows:

$$a_{ij} = \begin{cases} 1 & \text{if } SCI_{ij} > 1 \text{ and } i \neq j \\ 0 & \text{otherwise} \end{cases} \tag{2}$$

This implies that I treat ZCTA-pairs with an SCI value of 1 as not being socially connected, or not being neighbours in social space, whereas I deem ZCTA-pairs with SCI values above 1 as social neighbours. It further implies that I discard the social ties of each area with itself to focus on its relations with others, resulting in a zero-diagonal matrix. Recall that as SCI values are scaled to range between 1 and 1,000,000,000, ZCTA-pairs with a value of 1 have the lowest

[8]Note that this holds irrespective of how distant any given pair of ZCTAs are from each other.

pairwise density of social ties observed across the United States. While there is no available information on the actual density of social ties represented by a value of 1, the within-ZCTA distribution of SCI values is plausibly consistent with its interpretation as near-zero density. On average, an SCI value of 1 will characterise the social ties of an area with more than half of all others, with the next lower value being larger by a factor of 387, indicating a sharp decline to the global minimum. This empirical pattern echoes studies of personal social networks in large communities (e.g Fischer, 1982), suggesting that individuals tend to have a few first-degree social ties but are not directly tied to most others.

I combine information on the density of social ties and social neighbourhood relations by constructing a spatial weights matrix $\mathbf{W}$ with elements w_{ij} as follows:

$$w_{ij} = \begin{cases} SCI_{ij} & \text{if } a_{ij} = 1 \text{ and } SCI_{ij} \text{ is in } \min_i(\sum_j a_{ij}) \text{ highest in row} \\ 0 & \text{otherwise} \end{cases} \tag{3}$$

Intuitively, the above implies that I consider ZCTA-pairs that are social neighbours to be more proximate in social space when they have a higher density of social ties. It also implies that I only consider the social ties of each area with its 1,347 most connected social neighbours: the minimum number of neighbours across all areas. The latter approach has two advantages. First, by restricting all ZCTAs to have the same number of social neighbours, it improves comparability of social relations across areas. The choice of the minimum number of neighbours across all areas as the cut-off ensures that this is achieved while retaining the maximum amount of information on the social ties among them.[9] Second, it results in a sparse spatial weights matrix with a sparsity of 0.06: a desirable property in the computation of local Moran index, which is the preferred measure of partisan homophily discussed later in this section.

To examine the relative extent in which the population of a given ZCTA is socially connected to those of other ZCTAs, I calculate the relative connectedness to its social neighbours as follows:

$$RelConnSocNb_i = \frac{\sum_j SCI_{ij} \times \hat{w}_{ij}}{SCI_{ii}} \tag{4}$$

[9]Assuming that Facebook usage rates are similar across ZCTAs, on average, an estimated 74 per cent of the social ties of an area in all others lie in its 1,347 social neighbours.

Here, $\hat{w}_{ij}$ represents elements from the row-normalised version of the weights matrix $\mathbf{W}$ identifying the social neighbours of each ZCTA, and SCI_{ii} represents the density of social ties within the population of each ZCTA, i. That is, the relative connectedness of a ZCTA with its social neighbours is the mean social connectedness to its social neighbours over its social connectedness to itself. As such, higher values of this measure suggest that the population of the ZCTA in question has more of its social ties located in other ZCTAs.

To examine the relative extent in which the non-local social ties of the population of a given ZCTA are geographically distant, I calculate the relative distance to social neighbours as follows:

$$RelDistSocNb_i = \frac{\sum_j d_{ij} \times SCI_{ij} \times \hat{w}_{ij}}{\sum_j d_{ij} \times \hat{g}_{ij}} \tag{5}$$

Here, d_{ij} represents the great-circle geographic distance between a ZCTA-pair ij, and $\hat{g}_{ij}$ represents elements from the row-normalised version of the weights matrix $\mathbf{G}$, which identifies the geographic neighbours of each ZCTA excluding itself.[10] That is, the relative distance of a ZCTA from its social neighbours is the SCI-weighted great-circle distance to its social neighbours over the mean distance to its geographic neighbours. Consequently, higher values of this measure denote that the non-local social ties of the population of the ZCTA in question are less likely to be located in geographically proximate areas.

Panel A of Figure 1 maps the log of relative connectedness to social neighbours. It is shown that, on average, the populations of ZCTAs which are closer to population centres are more likely to have more of their social ties in other ZCTAs. Panel B also maps the log of relative distance to social neighbours. This further suggests that, on average, the non-local social ties of ZCTAs that are closer to population centres are less likely to be located in geographically proximate areas. Taken together, these patterns appear consistent with the 'community liberated' argument in urban sociology (e.g. see Wellman, 1979), which contends that urbanites maintain more sparsely knit, spatially dispersed networks relative to the

[10] Mirroring the definition of social neighbours, geographic neighbours are defined as the 1,347 most geographically proximate ZCTAs in the data. Standardising the distance to social neighbours by that to geographic neighbours accounts for the fact that the former could, in relative terms, be artificially inflated by missing data or features of the population geography of the US. Appendix Figure A.3 offers a mapped comparison of the respective standardised and unstandardised measures, showing that ZCTAs where standardisation results in increases in the relative distance to social neighbours are primarily located in the Midwest and the Northeast, while the ZCTAs that see the largest decreases are located in the South and West.

inhabitants of rural areas. However, the maps are also suggestive of substantial regional heterogeneity, with several areas that are close to population centres in the more remote regions of the West, for instance, being socially connected to relatively more proximate areas.

2.2 Voting Data

Given that official election results are not published for ZCTAs, which is the level at which the data on social ties is available, I obtain 2020 US presidential election results at the precinct level. Namely, I use the dataset compiled by the Voting and Election Science Team (2020) of the University of Florida and Wichita State University, which includes information on precinct boundaries.

While most precincts fall entirely within a single ZCTA, nearly half of them do not. In order to harmonise the data on voting and social ties, I aggregate the former to the ZCTA level in three steps. First, I retrieve the spatial intersections between precinct and ZCTA polygons.[11] I then compute the percentage of the population of each ZCTA that is in each intersection using the High Resolution Settlement Layer (HRSL): a detailed, publicly available, 30-metre population grid produced by the Facebook Connectivity Lab and the Center for International Earth Science Information Network (CIESIN).[12] Finally, I use the derived population weights to apportion the precinct-level votes for each presidential candidate to each ZCTA.

In principle, to the extent that electoral support for any given presidential candidate is unevenly spatially distributed within any precinct spanning more than a single ZCTA, using population counts to apportion votes from such a precinct to intersecting ZCTAs can give rise to measurement error. However, other than the fact that fewer than half of precincts span multiple ZCTAs, there are two further points assuaging this concern. First, even within these precincts, the population overwhelmingly resides in a single ZCTA: on average, 78 per cent of the population of a precinct spanning ZCTAs falls within a single ZCTA. These precincts are also fairly homogeneous in terms of voting behaviour with an average of almost 70 per cent of the local vote being cast in favour of the leading candidate. Taken together, these points suggest that any measurement error arising from within-precinct variation in voting behaviour across ZCTA boundaries is unlikely to be substantial in the vast majority of cases.

[11] I use the 'tigris' R package by Walker and Rudis (2023) to obtain US Census Bureau shapefiles.
[12] The HRSL is distributed via the Humanitarian Data Exchange of the United Nations Office for the Coordination of Humanitarian Affairs.

Figure 1: Relative Connectedness and Distance to Social Neighbours, by ZCTA

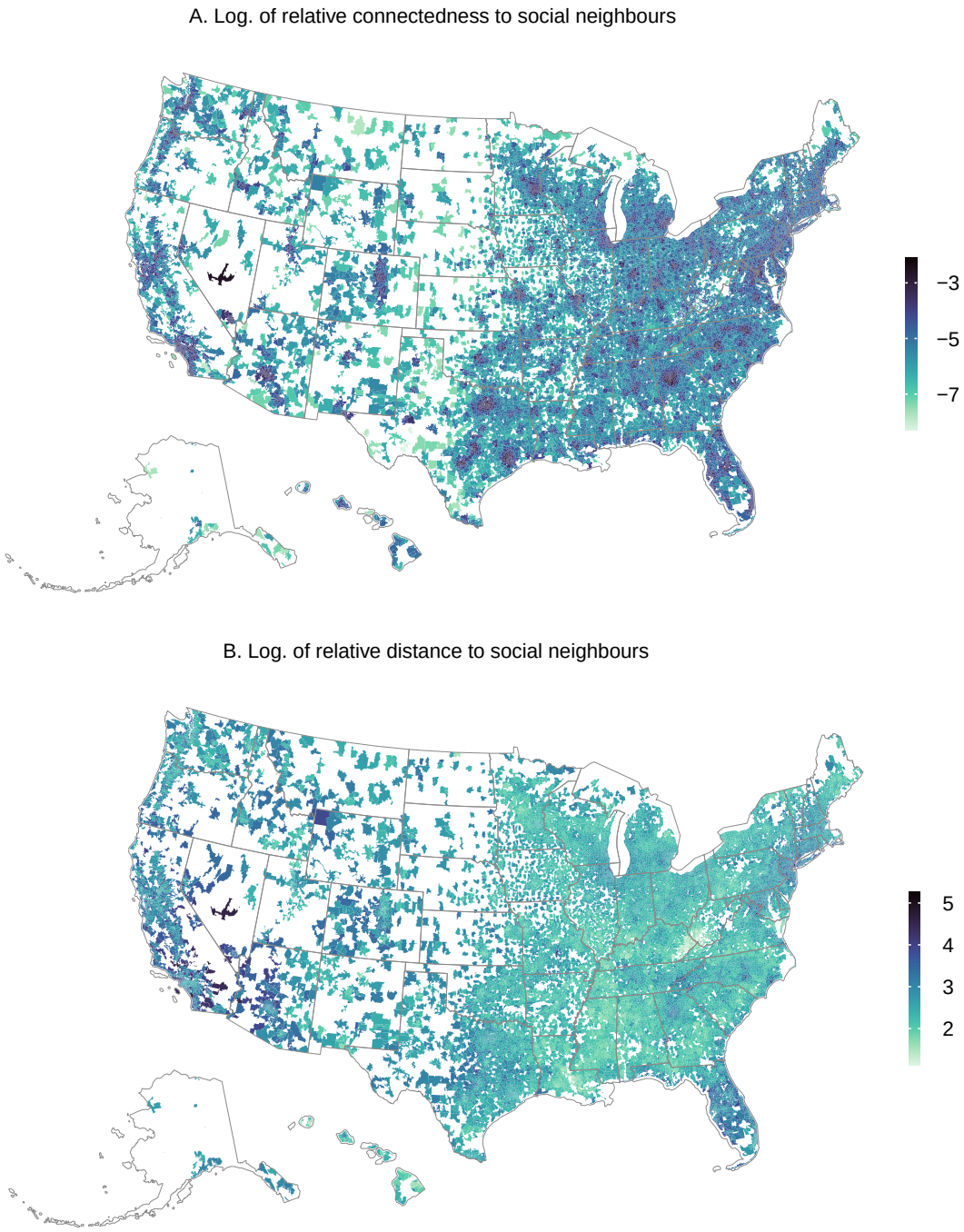

Notes: SCI refers to the Social Connectedness Index by Bailey et al. (2020). The social neighbours of a ZCTA are the 1,347 most socially connected ZCTAs to it as measured by the SCI. The relative connectedness of a ZCTA to its social neighbours is the mean SCI with its neighbours over the SCI within itself. The relative distance of a ZCTA to its social neighbours is the SCI-weighted great-circle distance to its social neighbours over the mean distance to its geographic neighbours.

I measure the partisan leaning of each area by calculating the Democratic two-party vote share in the 2020 US presidential election as follows:

$$r_i(D) = \frac{v_i(D)}{v_i(D) + v_i(R)} \tag{6}$$

Here, $r_i(D)$ is the Democratic two-party vote share in ZCTA i, with $v_i(D)$ and $v_i(R)$ respectively corresponding to votes for the Democratic presidential candidate, Joe Biden, and the Republican presidential candidate, Donald Trump. As such, high values of $r_i(D)$ indicate a strong Democratic leaning, with low values indicating a strong Republican leaning. Figure 2 maps the measure, reflecting the well-documented pattern of strong Democratic support in population centres. Note that $r_i(D)$ can also be thought of as a measure of partisan homogeneity, with values closer to 0.5 indicating heterogeneity in voting behaviour.

While the two-party vote share is often preferred as a straightforward measure of both partisan leaning and partisan homogeneity, it is important to note that it disregards votes for presidential candidates that are not affiliated with any the two major political parties. In principle, this measure could then be misleading in cases where a high share of local votes are cast in favour of such 'independent' candidates. However, such cases are exceedingly rare in practice: on average, in the 2020 US presidential election, 1.7 per cent of votes within a ZCTA were cast in favour of independent candidates, with over 95 per cent of ZCTAs seeing independent vote shares of below 5 per cent.[13] Appendix Figure A.2 maps independent vote shares across ZCTAs, showing that these are fairly even distributed in geographic space.

2.3 Demographic Data and Settlement Classification

I use 5-year estimates from the American Community Survey (ACS) produced by the US Census Bureau to observe a series of demographic characteristics of ZCTA populations as of 2020.[14] I further obtain information on the type of settlement best describing each ZCTA by using the Locale Assignments File produced by the National Centre for Education Statistics (NCES) (Geverdt, 2019).

[13] I use the term 'independent' to refer to both unaffiliated presidential candidates and candidates affiliated with parties other than the Democratic and Republican parties.

[14] I use the 'tidycensus' R package by Walker and Herman (2023) to obtain demographic data from the US Census Bureau application programming interface (API).

Figure 2: Democratic Two-Party Vote Share in the 2020 Presidential Election, by ZCTA

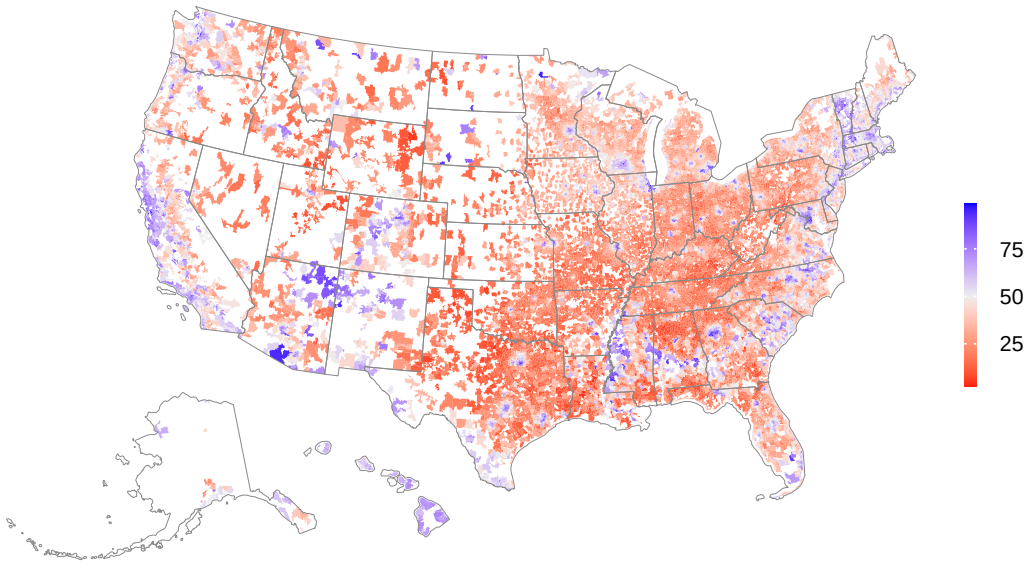

Notes: ZCTA-level vote shares are obtained by first apportioning precinct-level election results using the High Resolution Settlement Layer (HRSL).

The NCES framework offers a rarely detailed settlement classification at the ZCTA level. This is achieved by deriving classes based on both the extent in which ZCTA populations reside in different broad types of settlement as these are defined by official bodies—rural areas, urban clusters, urbanised areas, and principal cities—as well as their geographic distance from these types of settlement. A detailed description of the official definitions of settlements used in deriving the NCES classification is given by Geverdt (2018). Rural areas, urban clusters, and urbanised areas are defined by the US Census Bureau and are constructed from Census tracts and blocks. Urbanised areas are those containing 50,000 or more people, urban clusters are those containing more than 2,500 and less than 50,000 people, while rural areas are those outside urbanised areas and urban clusters.[15] Similarly, principal cities are defined by the US Office of Management and Budget and correspond to incorporated and Census-designated places within core based statistical areas. While there are several alternative qualifying criteria, these generally require that a place has a resident population of at least 10,000 people and a substantial number of workers from other places.

[15]In 2020, the US Census Bureau defined both urbanised areas and urban clusters as 'urban areas'. The NCES classification framework is thus based on definitions as of the 2010 Census.

At the lowest level, the NCES classification is comprised of 14 classes. For brevity, I use an aggregated version of the classification comprised of the following 5 classes, which are also mapped on Figure 3:

- *City*: Territory inside an urbanised area and inside a principal city.
- *Suburb*: Territory outside a principal city and inside an urbanised area.
- *Rural – Fringe*: Census-defined rural territory that is less than or equal to 5 miles from an urbanised area, or rural territory that is less than or equal to 2.5 miles from an urban cluster, or territory inside an urban cluster.[16]
- *Rural – Distant*: Census-defined rural territory that is more than 5 miles but less than or equal to 25 miles from an urbanised area, or is more than 2.5 miles but less than or equal to 10 miles from an urban cluster.
- *Rural – Remote*: Census-defined rural territory that is more than 25 miles from an urbanised Area and also more than 10 miles from an urban cluster.

Figure 3: ZCTA Settlement Type Classification

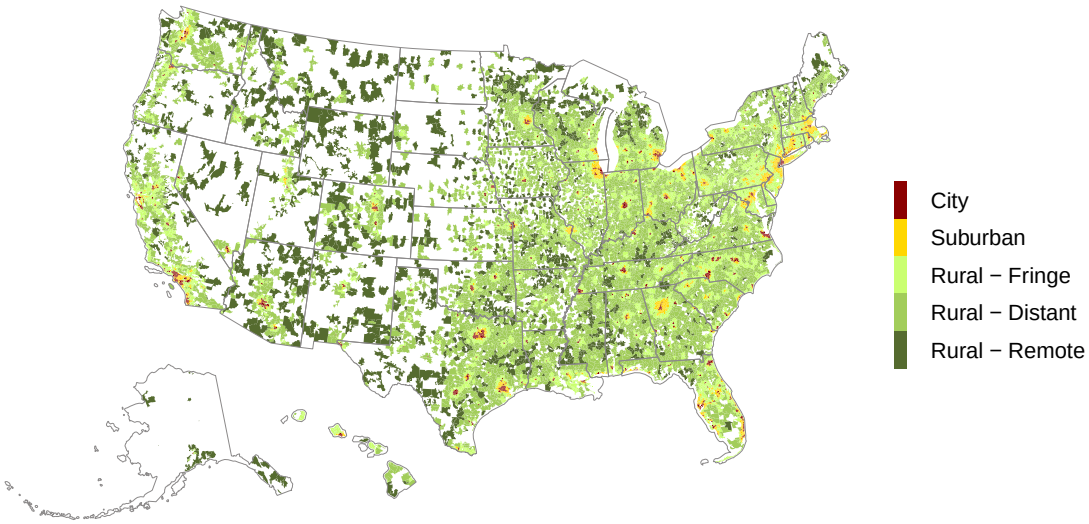

Notes: Settlement types are derived from the NCES Locale Assignments File (Geverdt, 2019)

[16]Territories inside urban clusters are classified as 'towns' by NCES. As very few ZCTAs fall under this class, I merge these with the related 'rural fringe' class. The latter is preferred over suburbs as urban clusters are generally much more distant relative to principal cities.

2.4 Identifying Politically Homophilous Clusters

In gauging whether there is evidence of partisan homophily or heterophily in each ZCTA, I use the local Moran index (Anselin, 1995): a popular local indicator of spatial association commonly employed in studies of partisan segregation (e.g. Darmofal and Strickler, 2019; Kinsella et al., 2021, 2015). However, unlike these studies, this paper is primarily concerned with the arrangement of voters in social space (homophily) rather than geographic space (segregation). This mandates a different approach in operationalising the interactions between disparate locations.

I compute the local Moran index for the Democratic two-party vote share in the 2020 US presidential election in each ZCTA as follows:[17]

$$I_i = \frac{z_i \sum_j \hat{w}_{ij} z_j}{\sum_i z_i^2} \tag{7}$$

Here, i and j index disparate ZCTAs, $\hat{w}_{ij}$ denotes elements of the row-standardised version of the spatial weights matrix $\mathbf{W}$ defined in (1), and z_i represents the standardised Democratic two-party vote share in i. What makes I_i interpretable as a local measure of partisan homophily rather than segregation is the way $\mathbf{W}$ is constructed. Rather than being populated on the basis of geographic distance between ZCTA-pairs, its elements are based on the pairwise density of social ties.

In standardising vote shares, I employ the Empirical Bayes (EB) approach proposed by Assunção and Reis (1999) as follows:[18]

$$z_i = \frac{r_i(D) - \beta}{\sqrt{\alpha + (\beta \div T_i)}} \tag{8}$$

In the above, $r_i(D)$ is the Democratic two-party vote share in area i, T_i is the total number of two-party votes cast in i, with β and α respectively denoting the empirically estimated mean and variance of a prior Gamma distribution.[19] The EB approach reflects the intuition that, insofar as the number of votes cast vary considerably across ZCTAs, the Democratic two-party vote share may be a relatively less precise estimate of the underlying partisan leaning in ZCTAs were few votes were cast. As this would violate the assumption of constant variance across locations in the calculation of the local Moran index, the standardisation of shares as in (8) serves to account for such cases.

[17] I use the 'spdep' R package by Bivand (2022) to calculate local Moran statistics.
[18] I use the 'rgeoda' R package by Li and Anselin (2023) to calculate EB shares.
[19] More specifically, $\beta = \sum_i v_i(D) \div \sum_i T_i$ and $\alpha = [\sum_i T_i (r_i(D) - \beta)^2] \div T - \beta \div (T \div n)$ where $v_i(D)$ is the number of democratic votes in i and n is the number of observations.

In effect, by computing the local Moran index as in (7), I conceptualise partisan homophily as positive autocorrelation in voting behaviour in social space. As is the case with operationalisations of the index as a measure of autocorrelation in geographic space, the main utility of this approach is that it facilitates significance testing against the null of no autocorrelation. As proposed by Anselin (1995), I do so by using a conditional permutation approach. Note that this departs from conventional notions of statistical significance in that pseudo p-values are obtained from simulated, empirical distributions of the index at each location.[20] Note further that the probability of false positives increases with the number of locations (de Castro and Singer, 2006), necessitating the downward adjustment of any pre-selected significance cut-off. I thus derive a critical p-value using the false discovery rate (FDR) criterion proposed by Benjamini and Hochberg (1995), setting the significance cut-off parameter to 0.05. With 22,537 locations, critical p-values derived in this way can be as low as $\frac{0.05}{22{,}537} = 2.2 \times 10^{-6}$. In order to allow for the detection of pseudo p-values below this threshold, I construct the simulated local distributions of the local Moran index using 499,999 permutations. After identifying locations where values of the local Moran index are significant, I assign them to politically homophilous and heterophilous clusters defined using the popular local Moran scatterplot approach discussed by Anselin (1995, 1996).

Locations with above and below-mean Democratic two-party vote shares $r_i(D)$ that respectively have social neighbours with above and below-mean SCI-weighted Democratic two-party vote shares $\sum_j \hat{w}_{ij} r_i(D)$ are assigned to two respective homophilous clusters—'High-High' and 'Low-Low'—and locations where the opposite relations hold are respectively assigned to two heterophilous clusters—'High-Low' and 'Low-High'. As such, the former group areas of similar partisan leaning where there is evidence of positive autocorrelation in voting behaviour in social space, and the latter represent areas where there is evidence of negative autocorrelation.

2.5 Examining the Determinants of Cluster Membership

To examine the ZCTA-level features associated with the various politically homophilous and heterophilous clusters, I employ a set of multinomial logistic specifications. I model the probability that ZCTA i is assigned to a cluster c as:

$$P_{ic} = \frac{e^{x_i' \beta_c}}{\sum_{k=1}^{m} e^{x_{ic}' \beta_{kc}}} \qquad \text{for} \quad c = 1, ..., m \tag{9}$$

[20] I describe values of the local Moran index as 'significant' when these correspond to pseudo p-values beyond a specified critical value along their local simulated distributions. As suggested by Efron and Hastie (2016), these values may be instead thought of as 'interesting'.

Here, x_i' is a vector of covariates and c indexes one of five categories: the High-High, Low-Low, High-Low, and Low-High local Moran clusters as well as a 'not significant' category for cases where there is insufficient evidence of homophily or heterophily. Typically, the odds ratio e^{β_c} capturing the marginal impact of each variable on the relative probability of belonging to category c as opposed to some other category c' can be obtained by normalising the coefficient $\beta_{c'}$ to zero. Though this can lead to difficulties in interpreting effects across categories, and can quickly become unwieldy in more complex specifications. I instead report the fitted probabilities $\hat{P}_{ic}$ and their respective 95% confidence intervals using the approach of Fox and Andersen (2006),[21] which can be straightforwardly interpreted as the probability that i is assigned to c for particular values of the covariates.

3 Results

Figure 4 shows the spatial distribution of local Moran clusters across ZCTAs. High-High and High-Low clusters represent areas with a relatively higher Democratic two-party vote share in the 2020 US presidential election and were, respectively, relatively more and less likely to be socially connected to areas with similar shares. Similarly, the Low-Low and Low-High clusters are comprised of areas with a relatively more Republican leaning in voting behaviour that were respectively, and in relative terms, more politically homophilous and heterophilous. Also mapped are the areas for which there is relatively limited evidence of partisan homophily or heterophily in terms of aggregate social ties in other areas. Figure 5 further plots the share of all ZCTAs and the share of the total population that is occupied by each cluster and within each US region—the Midwest, Northeast, South, and West—along with their corresponding 95 per cent confidence intervals.[22]

There is evidence of either partisan homophily or heterophily in 67 per cent of all ZCTAs, representing a 77 share of the total population. Areas where the evidence is limited are more likely to be found in the Midwest than elsewhere, constituting 47 per cent of all areas in the region. This compares against a respective 30, 29, and 26 per cent in the West, South, and Northeast, suggesting a greater incidence of partisan homophily or heterophily across areas in these regions. There is also substantial spatial variation within regions: one is less likely to come across evidently homophilous or heterophilous areas in settlements around upstate New York in the Northeast, along the coastal plains in the South, and away from the coast in the West than elsewhere in each respective region.

[21] I use the 'effects' R package by Fox and Weisberg (2019) to obtain the fitted probabilities and their confidence intervals.

[22] Appendix Table B.1 presents these results in table format.

Figure 4: Local Moran Clusters, by ZCTA

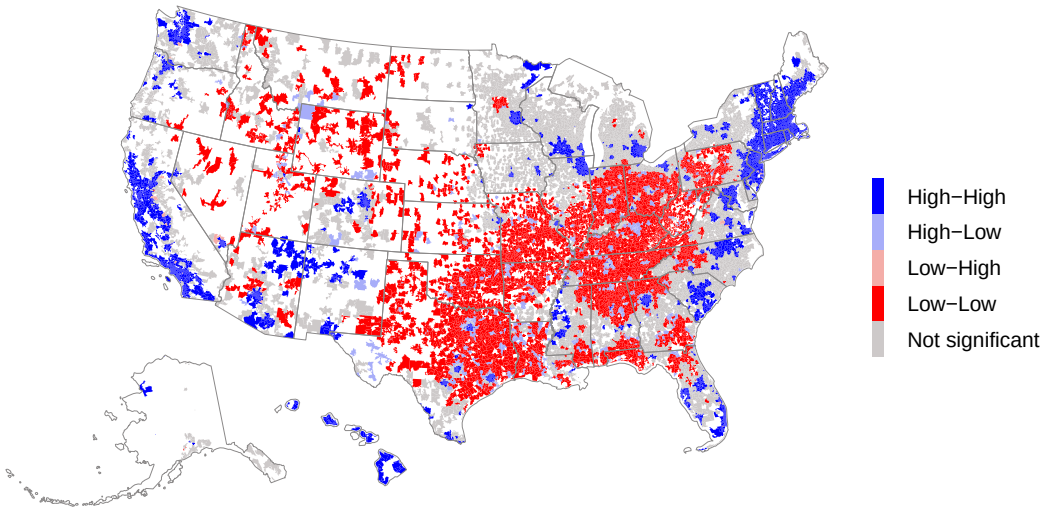

Notes: Local Moran index values measure autocorrelation in EB-standardised (Assunção and Reis, 1999) Democratic two-party vote shares as of the 2020 US presidential election, in the social space spanned by the 1,347 most connected areas as measured by the Social Connectedness Index (Bailey et al., 2020).

Figure 5: ZCTA and Population Shares, by Local Moran Cluster and Region

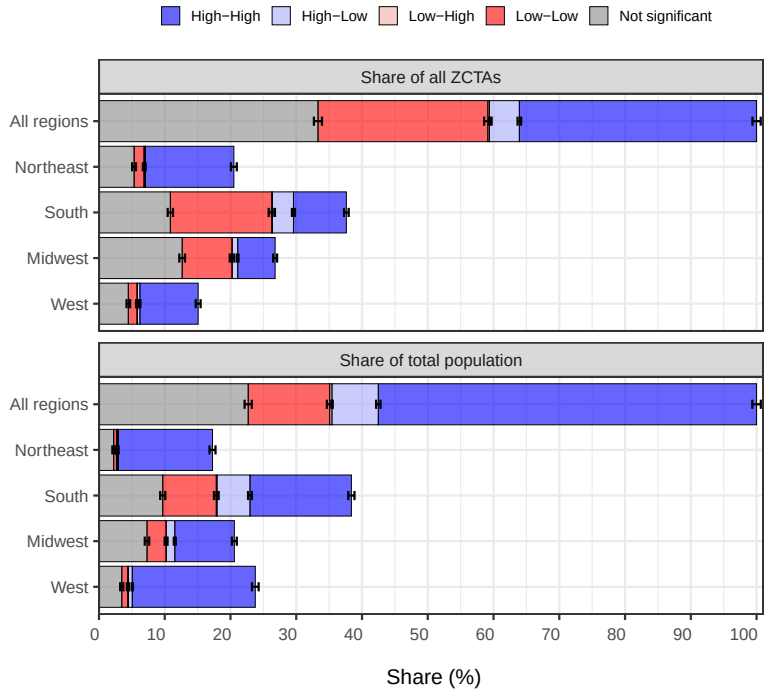

Notes: Black whiskers denote 95% confidence intervals. Local Moran index values measure autocorrelation in EB-standardised (Assunção and Reis, 1999) Democratic two-party vote shares as of the 2020 US presidential election, in the social space spanned by the 1,347 most connected areas as measured by the Social Connectedness Index (Bailey et al., 2020).

Despite not being evident in many areas, partisan homophily appears to be the norm across ZCTAs: homophilous areas account for roughly 70 per cent of the total population and all ZCTAs, with heterophilous areas accounting for 4.5 per cent of ZCTAs and 7 per cent of the population. Of the ZCTAs identified as politically homophilous or heterophilous, 57 per cent are Democratic-leaning, representing roughly 83 per cent of the population among these areas. The higher population share of Democratic-leaning areas relative to their share of ZCTAs is in line with the spatial concentration of Democrats around population centres.

Partisan heterophily is almost exclusively observed among Democratic-leaning areas, with just 0.24 per cent of all ZCTAs identified as Republican-leaning and heterophilous, representing 0.3 per cent of the total population. Interestingly, the share of the population in heterophilous Democratic-leaning areas relative to that in homophilous areas of the same leaning matches the respective share of ZCTAs at roughly 12 per cent. This suggests that there are no major differences in the spatial concentration of voters in homophilous and heterophilous Democratic-leaning areas. Further, looking at the regional distribution of heterophilous Democratic-leaning areas, it is shown that these are most common in the South and the Midwest. These are also the regions within which Democratic-leaning areas are the least spatially dispersed.

How does partisan homophily relate to urbanisation across regions? The first column of Figure 6 displays fitted probabilities from multinomial logistic specifications regressing local Moran cluster membership on the interaction of US region and settlement type as per the NCES classification.[23,24] On average, more urbanised settlements have a higher probability of belonging to a homophilous Democratic-leaning cluster and a lower probability of belonging to a homophilous Republican-leaning cluster. With the exception of areas in the South, the relative probability of being in a politically homophilous as opposed to neither a homophilous nor a heterophilous cluster also tends to decrease with urbanisation. Looking at the edges of the urban-rural continuum, a ZCTA in a city is 2.5 times more likely to be homophilous and Democratic-leaning than a remote rural area is likely to be homophilous and Republican-leaning. As such, when compared to rural areas, cities and suburbs are generally more likely to be politically homophilous when it comes to their aggregate social ties in other areas. Cities, suburbs, and rural fringes in the South are also the most likely areas to be Democratic-leaning and heterophilous with a probability of slightly over 10 per cent.

[23] I match each ZCTA to a parent county, state, and region using the 'Geocorr' application of the Missouri Census Data Centre, which provides correspondence tables based on the majority population share within each geography as of the 2020 Census.

[24] Appendix Table B.2 presents these results in table format.

Figure 6: Fitted Probability of Local Moran Cluster, by Region and Settlement Type

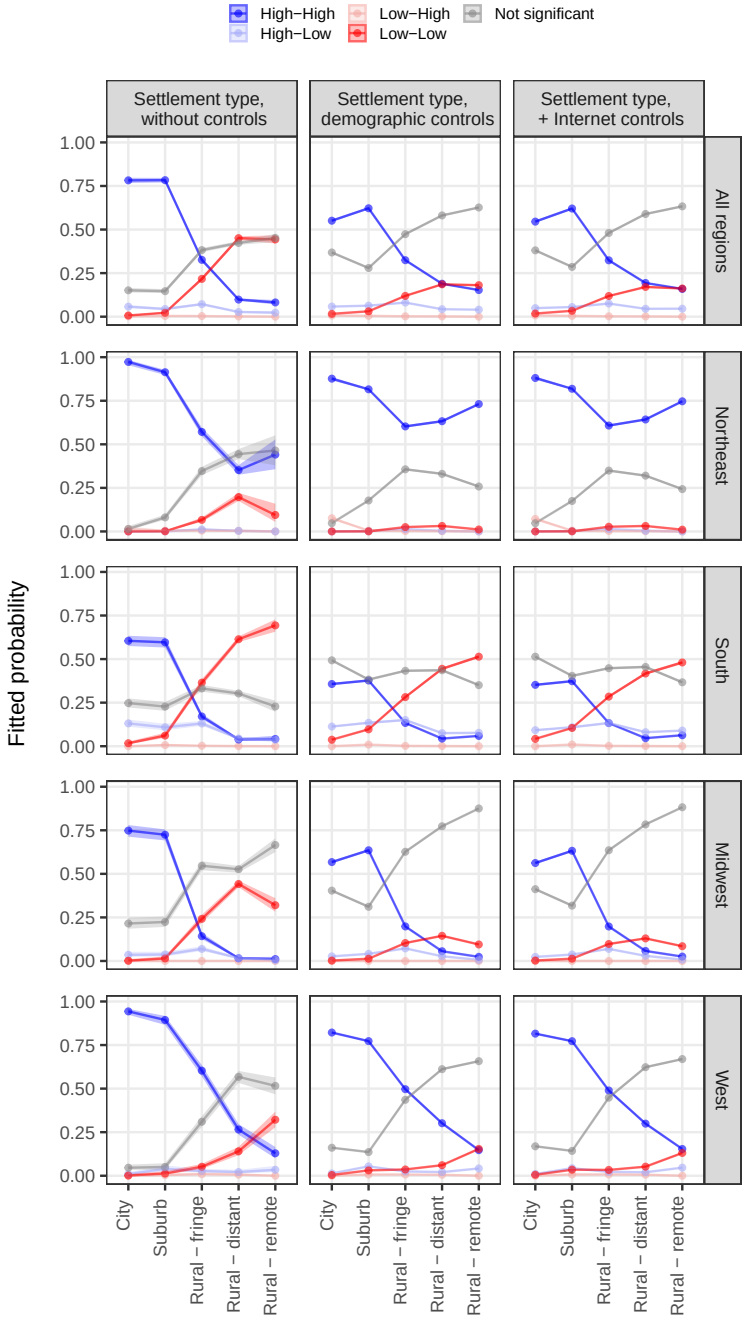

Notes: Each column corresponds to a multinomial logistic regression with cluster membership as the outcome. Points and shaded areas respectively correspond to fitted probabilities and 95% confidence intervals obtained using the approach of Fox and Andersen (2006). Local Moran index values measure autocorrelation in EB-standardised (Assunção and Reis, 1999) Democratic two-party vote shares as of the 2020 US presidential election, in the social space spanned by the 1,347 most connected areas as measured by the Social Connectedness Index (Bailey et al., 2020).

To what extent is the association between partisan homophily and urbanisation across regions explained by demographic characteristics? The second column of Figure 6 displays fitted probabilities from multinomial logistic specifications mirroring those of the first column while additionally controlling for ZCTA-level median age, median household income, white population share, the share of owner-occupied housing units, and the over 25 population share with a university degree. On average, a similar broad pattern holds: net of demographic characteristics, as urbanisation increases an area is more likely to be homophilous and Democratic-leaning and less likely to be homophilous and republic Republican leaning, with more urbanised settlements being more likely to be homophilous. However, compared to specifications without controls, the probability of being in neither a politically homophilous nor a heterophilous cluster gains an average of 16 percentage points across regions and settlements, suggesting that partisan homophily is at least partly explained by spatial variation in the demographic composition of different settlement types. This is most salient in cities of the South and rural areas of the Midwest, where the gain in probability stands at over 20 percentage points. Distant and remote rural areas of the Northeast are outliers in that the opposite holds: when accounting for demographic composition, the probability of such areas being politically homophilous increases by over 10 percentage points, with the probability of being homophilous and Democratic-leaning becoming higher than that in rural areas around urban fringes.

As discussed in the previous section, there is strong evidence that the SCI is a sound proxy for the density of both online and offline social ties between the populations of ZCTA-pairs. Still, to the extent that there is substantial variation in Facebook usage, it is in principle possible that the relationship between partisan homophily and urbanisation as observed in the first two columns of Figure 6 is less representative of ZCTAs where Facebook usage is low. In order to gauge this prospect, in the third column of Figure 6, I append controls for the ZCTA-level percentage of households that own a smartphone as well as the average Internet download speed as of 2020.[25] Reassuringly, when compared to the second column, it is shown that there is very little change in the estimates, suggesting that the observed relationships between partisan homophily and urbanisation are unlikely to be merely explained by spatial variation in social media usage.

[25]Like the demographic variables, data for both of these variables come from the American Community Survey (ACS). In the absence of ZCTA-level data on Facebook usage, the latter two variables are intended as proxies for the latter.

Figure 7: Fitted Probability of Local Moran Cluster, by Relative Connectedness and Distance to Social Neighbours

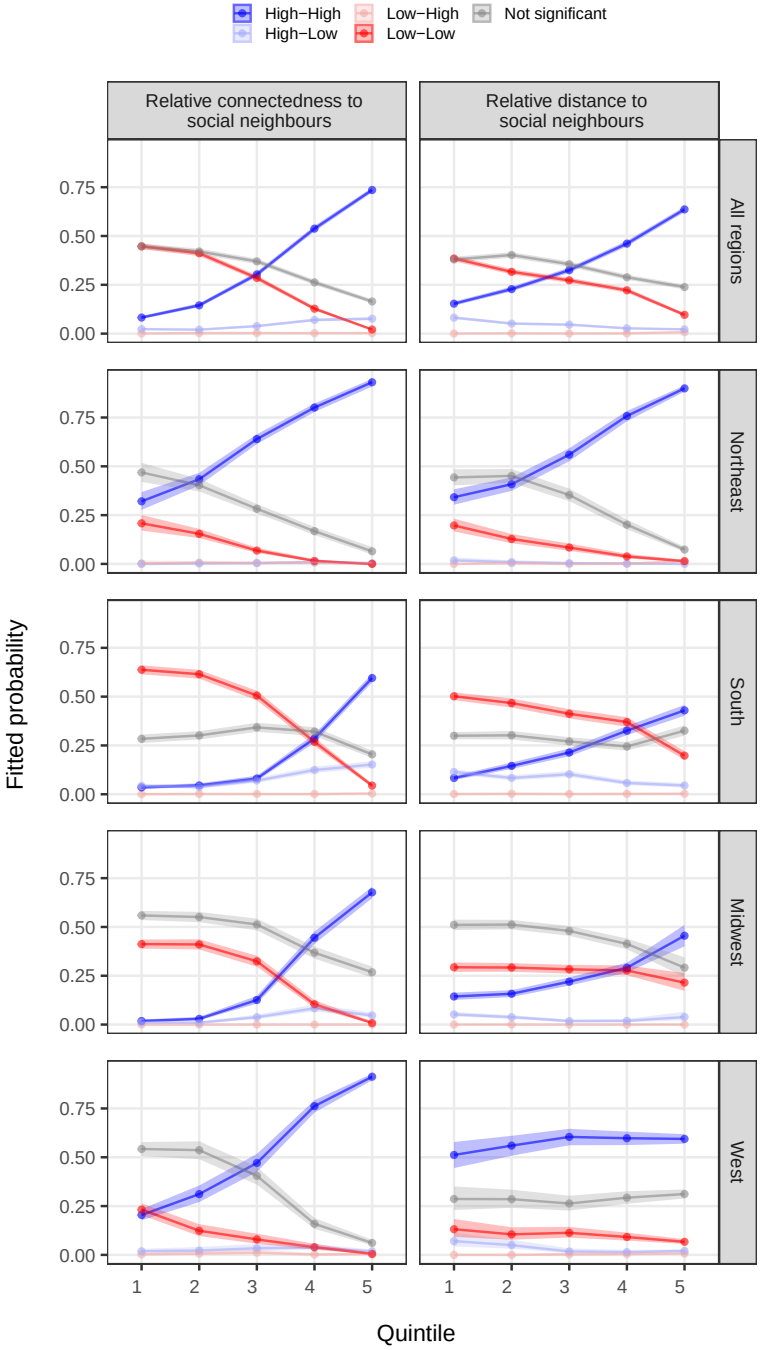

Notes: Each column corresponds to a multinomial logistic regression with cluster membership as the outcome. Points and shaded areas respectively correspond to fitted probabilities and 95% confidence intervals obtained using the approach of Fox and Andersen (2006). Local Moran index values measure autocorrelation in EB-standardised (Assunção and Reis, 1999) Democratic two-party vote shares as of the 2020 US presidential election, in the social space spanned by the social neighbours of each area: the 1,347 most connected areas as measured by the Social Connectedness Index (SCI) (Bailey et al., 2020).

Figure 7 presents fitted probabilities from multinomial logistic specifications regressing local Moran cluster membership respectively on quintiles of the relative connectedness and distance of each ZCTA to its social neighbours.[26] Looking at the first column, it is shown that, on average, as the relative connectedness of a ZCTA to its social neighbours increases, the probability that it is homophilous and Democratic-leaning increases. A politically homophilous area in the first quintile of relative connectedness, in which the density of social ties within the median area is 500 times higher than the mean density of its ties in other areas, is over 5 times more likely to be Republican-leaning. In contrast, a politically homophilous area in the fifth quintile, in which the within-density of social ties of the median area is 41 times higher than the mean density of its ties elsewhere, is 35 times more likely to be Democratic-leaning. Notably, the disproportionate increase in the relative probability of homophilous Democratic-leaning clusters in higher quintiles is in line with a decrease in the probability of an area being identified as neither homophilous nor heterophilous. In other words, areas with a higher relative density of social ties in others are both more likely to be politically homophilous and Democratic-leaning. There is further notable regional heterogeneity in the relationship between partisan homophily and the relative distance to social neighbours, with the latter being weaker for Midwestern and Southern ZCTAs in the first to third quintile of relative distance.

Looking at the second column of Figure 7, it is shown that there is also an overall positive relationship between the probability of a political homophilous area being Democratic-leaning and the relative distance to its social neighbours. In the first quintile of relative distance, in which the distance of the median area to its social neighbours is 3 times higher than the distance to its geographic neighbours, a politically homophilous area is 2.5 times more likely to be Republican-leaning rather than Democratic-leaning. In the fifth quintile, in which the distance to social neighbours is 26 times higher than the distance to its geographic neighbours, a homophilous area is 7 times more likely to be Democratic-leaning rather than Republican-leaning. While broadly similar patterns hold across US regions, the relationship between partisan homophily and relative distance to social neighbours appears weakest in the West, where increases in relative distance are associated with modest changes in the probability of membership across local Moran clusters when compared against those in other regions. In line with the discussion of Figure 1, this is likely to be partly due to greater heterogeneity in the relative distance to social neighbours among urban areas of the West.

[26] Appendix Table B.3 presents these results in table format.

4 Discussion and Conclusion

When examined in conjunction with the findings of studies on partisan segregation, the empirical results of this paper suggest that the geography of partisan homophily in the United States broadly tracks that of the latter. Perhaps the most direct comparison can be made with the findings of Darmofal and Strickler (2019): whereas in this paper partisan homophily is measured as autocorrelation in social space in voting behaviour in the 2020 US presidential election at the ZCTA level, the authors measure partisan segregation as autocorrelation in geographic space in voting behaviour in the 2016 US presidential election at the county level.[27] Broadly similar regional patterns emerge; both politically homophilous and segregated areas of a Republican leaning are most likely to be found in, around, and between Texas and Kentucky in the South, while their Democratic-leaning counterparts are most common along the Northeastern and Western coasts. A fairly close correspondence also emerges with the findings of Brown and Enos (2021), who measure individual-level exposure to Republicans in most American voters' residential environments using voter registration data as of June 2018.[28] Just as exposure to registered Republicans quickly lowers as one approaches urban cores, the probability of an area being Democratic-leaning in its voting behaviour in 2020 as well as having denser social ties in other areas that voted similarly becomes substantially higher. What is more, just as Democrats are, on average, less likely to be exposed to Republicans in their residential environment, politically homophilous areas are more likely to be Democratic-leaning rather than Republican-leaning.

Overall, the evidence presented in this paper supports a long-held expectation regarding the electoral geography of the United States, which has nevertheless remained largely untested at scale. That is, by and large, segregation by partisanship in geographic space does go hand in hand with segregation by partisanship in social space. With the majority of ZCTAs across the United States identified as exhibiting a degree of partisan homophily with respect to their aggregate social ties in other areas, it thus seems likely that the prevalence of partisan homophily is a relevant factor in the rise of affective and ideological polarisation in the country in recent years. As is the case with spatial variation in voting behaviour (Scala and Johnson, 2017), the position of voters along the urban-rural continuum also appears to play an important role in spatial variation in partisan homophily that goes beyond differences in the demographic composition of local populations.

[27] For Darmofal and Strickler (2019), two counties are considered as geographic neighbours when they are contiguous.

[28] In calculating individual-level exposure to Republicans, Brown and Enos (2021) consider the thousand nearest neighbours in terms of residence.

Crucially, this paper also highlights a relatively neglected prospect in the empirical electoral geography literature, relating to the wider uncertain geographic context problem (Kwan, 2012; Fowler et al., 2020). While social contextual influences on political preference formation are typically equated to aggregate socioeconomic conditions within the localities in which voters are resident (Ethington and McDaniel, 2007; Gimpel and Reeves, 2022; Johnston and Pattie, 2014), the evidence presented in this paper shows that this may systematically conceal the relevance of non-local context in certain kinds of localities. Indeed, when compared to voters in areas with a strong Republican leaning—which are most likely to be rural—voters in areas with a strong Democratic leaning—which are most likely to be cities and suburbs—are more likely to be socially connected to co-partisans in distant areas. The implications of this finding become clear in light of the evidence on the political effects of exposure to heterogeneous urban environments (e.g. Enos, 2017) and the importance of co-partisan ties in political preference formation in the United States (e.g. Huckfeldt and Sprague, 1995). As discussed by Baybeck and Huckfeldt (2002a,b), while social ties with non-local co-partisans may not expose voters to politically divergent contexts, they may act as channels via which information about non-local socioeconomic shocks feeds into local political preferences. Consequently, the finding that such long-distance spillovers are likely to be especially relevant to political outcomes within urban, Democratic-leaning areas, points to a promising avenue of research on their role in shaping the electoral geography of the United States, in line with similar work in other domains (Charoenwong et al., 2020; Holtz et al., 2020; Makridis, 2022; Wilson, 2022; Zhao et al., 2021).[29]

The findings also suggest that the 2020 US presidential election saw differences in the regional distribution of politically homophilous areas and spatial heterogeneity in the relationship between partisan homophily on the one hand and settlement type and network features on the other. A substantial share of areas representing as much as a fifth of the total population were identified as neither homophilous nor heterophilous, with the majority being distributed in the South and the Midwest. Also most common in these regions were the few heterophilous areas that were more likely to be socially connected to politically dissimilar others, primarily represented by Demoratic-leaning areas along urban fringes with relatively geographically proximate social ties. In addition, the findings highlighted the presence of important regional heterogeneity. For instance, contrary to rural areas in other regions, rural areas of the Northwest were shown to be more likely to be homophilous and Democratic-leaning the further away these were from urban

[29]This is also informative with respect to the potential externalities of proposed policy responses to political polarisation, such as compulsory voting in blue states (Rodden, 2015).

fringes. Similarly, it was shown that the relationship between partisan homophily and the relative distance of co-partisan social ties was weaker in the West than elsewhere. As such, researchers interested in political preferences in particular regions and settlements should be cautious of this heterogeneity.

Examining the geography of partisan homophily on the basis of voting behaviour in the 2020 US presidential election aids with the task of maximising correspondence between the dates and geographies for which partisanship and social ties are observed. As spatial patterns in voting behaviour are likely to change over time, it is important to note that developing a better understanding of how this geography evolves will require revisiting its measurement as more relevant data become available. While there are a number of barriers in their collation for all localities, voter registration data could also plausibly improve measurement, given that registered partisan affiliation may offer a more explicit indicator of partisan identity than voting behaviour.

Finally, recall that, in line with data availability, this paper has examined partisan homophily in terms of the aggregate social ties between ZCTAs. Though partisan homophily is also likely to vary within these localities: a prospect that is arguably reinforced given the evidence on variation in partisan segregation at very fine spatial resolutions (Brown and Enos, 2021). Indeed, the empirical analysis has shown that while there is substantial spatial variation in the degree in which the density of social ties within a ZCTA exceeds the mean density of its social ties in others, the latter is, on average, dwarfed by the former. However, as argued in this paper, this variation may still play an important role in the formation of political preferences insofar as it represents differences in the flow of information between disparate, or even distant areas. As anticipated by Granovetter (1973, 1983), influence and information often diffuse through 'weak ties' bridging otherwise disconnected groups of individuals.

Appendix

A Additional Figures

Figure A.1: Availability of the Social Connectedness Index, by ZCTA

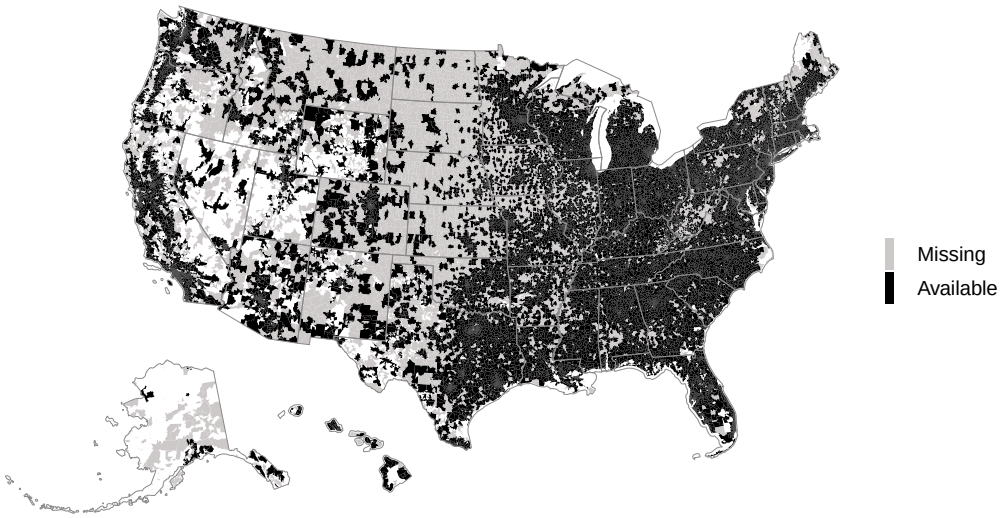

Figure A.2: Independent Vote Share, 2020 Pres. Election, by ZCTA

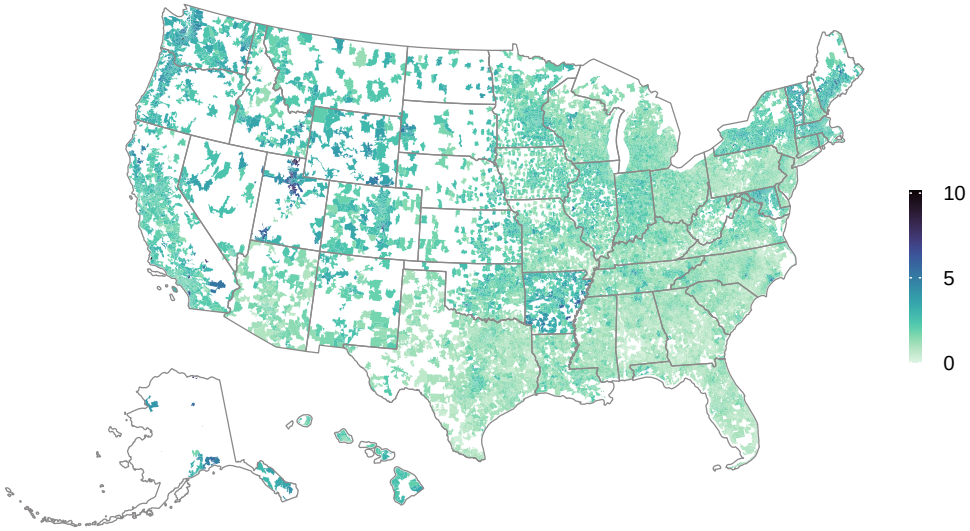

Notes: The term 'independent' refers to candidates that are either unaffiliated or not affiliated with the Democratic or the Republican party.

Figure A.3: Change in Quintile Rank from Standardisation of Distance to Social Neighbours, by ZCTA

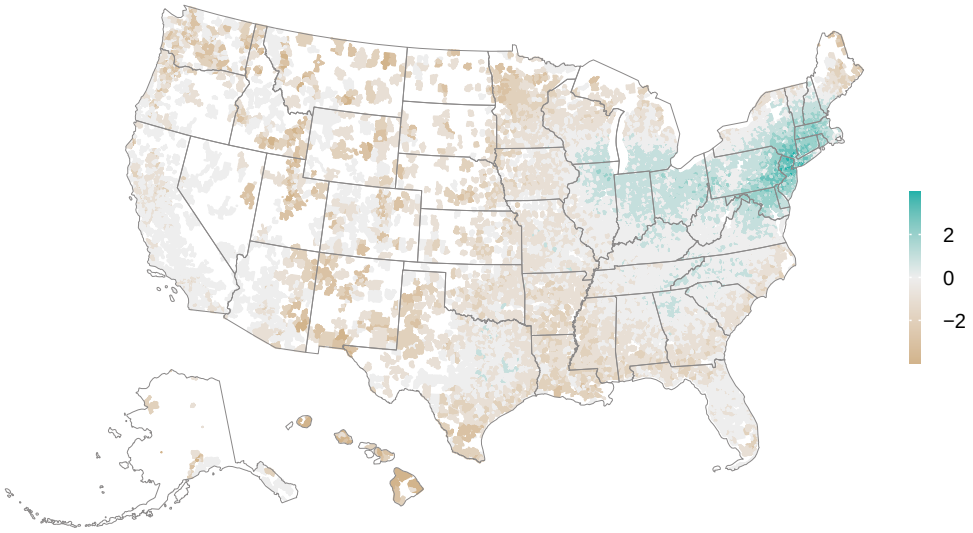

Notes: The map is coloured by the ZCTA-level difference between the quintile rank of the SCI-weighted great-circle distance to social neighbours and the quintile rank of the latter measure after standardisation by the mean distance to geographic neighbours.

B Additional Tables

Table B.1: ZCTA and Population Share, by Local Moran Cluster and Region

A. *Share of all ZCTAs (%)*					
	High-High	High-Low	Low-High	Low-Low	Not sig.
All regions	36.07	4.55	0.24	25.84	33.3
	(0.32)	(0.14)	(0.03)	(0.29)	(0.31)
Northeast	13.48	0.1	0.1	1.5	5.34
	(0.23)	(0.02)	(0.02)	(0.08)	(0.15)
South	8.04	3.22	0.07	15.43	10.85
	(0.18)	(0.12)	(0.02)	(0.24)	(0.21)
Midwest	5.69	0.86	0	7.58	12.65
	(0.15)	(0.06)	(0)	(0.18)	(0.22)
West	8.86	0.37	0.07	1.32	4.46
	(0.19)	(0.04)	(0.02)	(0.08)	(0.14)
B. *Share of total population (%)*					
	High-High	High-Low	Low-High	Low-Low	Not sig.
All regions	57.52	7.06	0.33	12.4	22.69
	(0.33)	(0.17)	(0.04)	(0.22)	(0.28)
Northeast	14.33	0.13	0.14	0.43	2.23
	(0.23)	(0.02)	(0.03)	(0.04)	(0.1)
South	15.43	5.01	0.11	8.15	9.69
	(0.24)	(0.15)	(0.02)	(0.18)	(0.2)
Midwest	9.06	1.31	0	2.91	7.3
	(0.19)	(0.08)	(0)	(0.11)	(0.17)
West	18.71	0.6	0.08	0.91	3.46
	(0.26)	(0.05)	(0.02)	(0.06)	(0.12)

Notes: Standard errors are shown in parentheses. Local Moran index values measure autocorrelation in EB-standardised (Assunção and Reis, 1999) Democratic two-party vote shares as of the 2020 US presidential election, in the social space spanned by the 1,347 most connected areas as measured by the Social Connectedness Index (Bailey et al., 2020).

Table B.2: Fitted Probability of Local Moran Cluster, by Region and Settlement Type

A. *Without controls*					
	High-High	High-Low	Low-High	Low-Low	Not sig.
All regions					
City	0.78	0.06	0	0.01	0.15
	(0.01)	(0.00)	(0.00)	(0.00)	(0.01)
Suburb	0.78	0.04	0	0.02	0.15
	(0.01)	(0.00)	(0.00)	(0.00)	(0.01)
Rural - fringe	0.33	0.07	0	0.22	0.38
	(0.01)	(0.00)	(0.00)	(0.01)	(0.01)
Rural - distant	0.1	0.03	0	0.45	0.42
	(0.00)	(0.00)	(0.00)	(0.01)	(0.01)
Rural - remote	0.08	0.02	0	0.44	0.45
	(0.01)	(0.00)	(0.00)	(0.01)	(0.01)
Northeast					
City	0.97	0	0.01	0	0.01
	(0.01)	(0.00)	(0.00)	(0.00)	(0.00)
Suburb	0.91	0	0	0	0.08
	(0.01)	(0.00)	(0.00)	(0.00)	(0.01)
Rural - fringe	0.57	0.01	0	0.07	0.35
	(0.01)	(0.00)	(0.00)	(0.01)	(0.01)
Rural - distant	0.35	0	0	0.2	0.44
	(0.01)	(0.00)	(0.00)	(0.01)	(0.01)
Rural - remote	0.44	0	0	0.09	0.46
	(0.04)	(0.00)	(0.00)	(0.02)	(0.04)
South					
City	0.6	0.13	0	0.02	0.25
	(0.02)	(0.01)	(0.00)	(0.00)	(0.01)
Suburb	0.6	0.11	0.01	0.06	0.23
	(0.02)	(0.01)	(0.00)	(0.01)	(0.01)
Rural - fringe	0.17	0.13	0	0.36	0.33
	(0.01)	(0.01)	(0.00)	(0.01)	(0.01)

(continued on next page)

Table B.2: (continued)

	High-High	High-Low	Low-High	Low-Low	Not sig.
Rural - distant	0.04	0.04	0	0.61	0.3
	(0.00)	(0.00)	(0.00)	(0.01)	(0.01)
Rural - remote	0.04	0.04	0	0.69	0.23
	(0.01)	(0.01)	(0.00)	(0.02)	(0.02)
Midwest					
City	0.75	0.04	0	0	0.22
	(0.02)	(0.01)	(0.00)	(0.00)	(0.02)
Suburb	0.72	0.04	0	0.01	0.22
	(0.02)	(0.01)	(0.00)	(0.00)	(0.01)
Rural - fringe	0.14	0.07	0	0.24	0.55
	(0.01)	(0.01)	(0.00)	(0.01)	(0.01)
Rural - distant	0.02	0.02	0	0.44	0.53
	(0.00)	(0.00)	(0.00)	(0.01)	(0.01)
Rural - remote	0.01	0	0	0.32	0.67
	(0.00)	(0.00)	(0.00)	(0.02)	(0.02)
West					
City	0.94	0.01	0	0	0.05
	(0.01)	(0.00)	(0.00)	(0.00)	(0.01)
Suburb	0.89	0.04	0	0.01	0.05
	(0.01)	(0.01)	(0.00)	(0.00)	(0.01)
Rural - fringe	0.6	0.03	0.01	0.05	0.31
	(0.01)	(0.00)	(0.00)	(0.00)	(0.01)
Rural - distant	0.27	0.02	0.01	0.14	0.57
	(0.02)	(0.00)	(0.00)	(0.01)	(0.02)
Rural - remote	0.13	0.03	0	0.32	0.52
	(0.01)	(0.01)	(0.00)	(0.02)	(0.02)

(continued on next page)

Table B.2: (continued)

B. *With demographic controls*					
	High-High	High-Low	Low-High	Low-Low	Not sig.
All regions					
City	0.55	0.06	0.01	0.02	0.37
	(0.00)	(0.00)	(0.00)	(0.00)	(0.00)
Suburb	0.62	0.06	0	0.03	0.28
	(0.00)	(0.00)	(0.00)	(0.00)	(0.00)
Rural - fringe	0.32	0.08	0	0.12	0.47
	(0.01)	(0.00)	(0.00)	(0.00)	(0.00)
Rural - distant	0.19	0.04	0	0.19	0.58
	(0.01)	(0.00)	(0.00)	(0.00)	(0.00)
Rural - remote	0.15	0	0.04	0.19	0.58
	(0.01)	(0.00)	(0.00)	(0.00)	(0.00)
Northeast					
City	0.88	0	0.08	0	0.05
	(0.01)	(0.00)	(0.00)	(0.00)	(0.00)
Suburb	0.82	0	0	0	0.18
	(0.00)	(0.00)	(0.00)	(0.00)	(0.00)
Rural - fringe	0.6	0.01	0	0.02	0.36
	(0.00)	(0.00)	(0.00)	(0.00)	(0.00)
Rural - distant	0.63	0	0	0.03	0.33
	(0.00)	(0.00)	(0.00)	(0.00)	(0.00)
Rural - remote	0.73	0	0	0.01	0.26
	(0.00)	(0.00)	(0.00)	(0.00)	(0.00)
South					
City	0.36	0.11	0	0.04	0.49
	(0.01)	(0.00)	(0.00)	(0.00)	(0.00)
Suburb	0.38	0.13	0.01	0.1	0.38
	(0.00)	(0.00)	(0.00)	(0.00)	(0.00)
Rural - fringe	0.13	0.15	0	0.28	0.43
	(0.00)	(0.00)	(0.00)	(0.00)	(0.00)

(continued on next page)

Table B.2: (continued)

	High-High	High-Low	Low-High	Low-Low	Not sig.
Rural - distant	0.04	0.08	0	0.44	0.44
	(0.00)	(0.00)	(0.00)	(0.00)	(0.01)
Rural - remote	0.06	0.08	0	0.51	0.35
	(0.00)	(0.00)	(0.00)	(0.00)	(0.00)
Midwest					
City	0.57	0.03	0	0	0.3
	(0.00)	(0.00)	(0.00)	(0.00)	(0.00)
Suburb	0.64	0.04	0	0.01	0.31
	(0.00)	(0.00)	(0.00)	(0.00)	(0.00)
Rural - fringe	0.2	0.07	0	0.1	0.63
	(0.00)	(0.00)	(0.00)	(0.00)	(0.00)
Rural - distant	0.06	0.03	0	0.14	0.77
	(0.00)	(0.00)	(0.00)	(0.00)	(0.00)
Rural - remote	0.02	0.01	0	0.09	0.88
	(0.00)	(0.00)	(0.00)	(0.00)	(0.00)
West					
City	0.82	0.01	0	0	0.16
	(0.00)	(0.00)	(0.00)	(0.00)	(0.00)
Suburb	0.77	0.05	0.01	0.03	0.14
	(0.00)	(0.00)	(0.00)	(0.00)	(0.00)
Rural - fringe	0.5	0.02	0.01	0.04	0.44
	(0.00)	(0.00)	(0.00)	(0.00)	(0.00)
Rural - distant	0.3	0.02	0.01	0.06	0.61
	(0.00)	(0.00)	(0.00)	(0.00)	(0.00)
Rural - remote	0.15	0.04	0	0.15	0.66
	(0.00)	(0.00)	(0.00)	(0.00)	(0.00)

(continued on next page)

Table B.2: (continued)

C. *With demographic and Internet controls*					
	High-High	High-Low	Low-High	Low-Low	Not sig.
All regions					
City	0.55	0.05	0.01	0.02	0.38
	(0.00)	(0.00)	(0.00)	(0.00)	(0.00)
Suburb	0.62	0.06	0	0.03	0.29
	(0.00)	(0.00)	(0.00)	(0.00)	(0.00)
Rural - fringe	0.32	0.08	0	0.12	0.48
	(0.01)	(0.00)	(0.00)	(0.00)	(0.00)
Rural - distant	0.19	0.05	0	0.17	0.59
	(0.01)	(0.00)	(0.00)	(0.00)	(0.00)
Rural - remote	0.16	0.05	0	0.17	0.59
	(0.01)	(0.00)	(0.00)	(0.00)	(0.00)
Northeast					
City	0.88	0	0.07	0	0.05
	(0.01)	(0.00)	(0.00)	(0.00)	(0.00)
Suburb	0.82	0	0	0	0.17
	(0.00)	(0.00)	(0.00)	(0.00)	(0.00)
Rural - fringe	0.61	0.01	0	0.03	0.35
	(0.00)	(0.00)	(0.00)	(0.00)	(0.00)
Rural - distant	0.64	0	0	0.03	0.32
	(0.00)	(0.00)	(0.00)	(0.00)	(0.00)
Rural - remote	0.75	0	0	0.01	0.24
	(0.00)	(0.00)	(0.00)	(0.00)	(0.00)
South					
City	0.35	0.09	0	0.04	0.51
	(0.01)	(0.00)	(0.00)	(0.00)	(0.00)
Suburb	0.37	0.11	0.01	0.1	0.4
	(0.00)	(0.00)	(0.00)	(0.00)	(0.00)
Rural - fringe	0.13	0.13	0	0.28	0.45
	(0.00)	(0.00)	(0.00)	(0.00)	(0.00)

(continued on next page)

Table B.2: (continued)

	High-High	High-Low	Low-High	Low-Low	Not sig.
Rural - distant	0.05	0.08	0	0.42	0.45
	(0.00)	(0.00)	(0.00)	(0.00)	(0.01)
Rural - remote	0.06	0.09	0	0.48	0.37
	(0.00)	(0.00)	(0.00)	(0.00)	(0.00)
Midwest					
City	0.56	0.02	0	0	0.41
	(0.00)	(0.00)	(0.00)	(0.00)	(0.00)
Suburb	0.63	0.04	0	0.01	0.32
	(0.00)	(0.00)	(0.00)	(0.00)	(0.00)
Rural - fringe	0.2	0.07	0	0.1	0.64
	(0.00)	(0.00)	(0.00)	(0.00)	(0.00)
Rural - distant	0.06	0.03	0	0.13	0.78
	(0.00)	(0.00)	(0.00)	(0.00)	(0.00)
Rural - remote	0.03	0.01	0	0.08	0.88
	(0.00)	(0.00)	(0.00)	(0.00)	(0.00)
West					
City	0.82	0.01	0	0.01	0.17
	(0.00)	(0.00)	(0.00)	(0.00)	(0.00)
Suburb	0.77	0.04	0.01	0.03	0.14
	(0.00)	(0.00)	(0.00)	(0.00)	(0.00)
Rural - fringe	0.49	0.02	0.01	0.03	0.45
	(0.00)	(0.00)	(0.00)	(0.00)	(0.00)
Rural - distant	0.3	0.02	0.01	0.05	0.62
	(0.00)	(0.00)	(0.00)	(0.00)	(0.00)
Rural - remote	0.15	0.05	0	0.13	0.67
	(0.00)	(0.00)	(0.00)	(0.00)	(0.00)

Notes: Panels A, B, and C each correspond to a multinomial logistic regression with cluster membership as the outcome. Fitted probabilities and standard errors (in brackets) are obtained using the approach of Fox and Andersen (2006). Local Moran index values measure autocorrelation in EB-standardised (Assunção and Reis, 1999) Democratic two-party vote shares as of the 2020 US presidential election, in the social space spanned by the 1,347 most connected areas as measured by the Social Connectedness Index (Bailey et al., 2020).

Table B.3: Fitted Probability of Local Moran Cluster, by Relative Connectedness and Distance to Social Neighbours

A. *Relative connectedness to social neighbours*					
	High-High	High-Low	Low-High	Low-Low	Not sig.
All regions					
1st quintile	0.08	0.02	0	0.45	0.45
	(0.01)	(0.00)	(0.00)	(0.01)	(0.01)
2nd quinitile	0.14	0.02	0	0.41	0.42
	(0.01)	(0.00)	(0.00)	(0.01)	(0.01)
3rd quintile	0.3	0.04	0	0.29	0.37
	(0.01)	(0.00)	(0.00)	(0.01)	(0.01)
4th quintile	0.54	0.07	0	0.13	0.26
	(0.01)	(0.00)	(0.00)	(0.00)	(0.01)
5th quintile	0.74	0.08	0	0.02	0.16
	(0.01)	(0.00)	(0.00)	(0.00)	(0.01)
Northeast					
1st quintile	0.32	0	0	0.21	0.47
	(0.02)	(0.00)	(0.00)	(0.02)	(0.02)
2nd quintile	0.43	0	0.01	0.15	0.4
	(0.02)	(0.00)	(0.00)	(0.01)	(0.02)
3rd quintile	0.64	0	0.01	0.07	0.28
	(0.01)	(0.00)	(0.00)	(0.01)	(0.01)
4th quintile	0.8	0.01	0.01	0.02	0.17
	(0.01)	(0.00)	(0.00)	(0.00)	(0.01)
5th quintile	0.93	0	0	0	0.06
	(0.01)	(0.00)	(0.00)	(0.00)	(0.01)
South					
1st quintile	0.03	0.04	0	0.64	0.28
	(0.00)	(0.00)	(0.00)	(0.00)	(0.01)
2nd quinitile	0.05	0.04	0	0.61	0.3
	(0.00)	(0.00)	(0.00)	(0.01)	(0.01)
3rd quintile	0.08	0.07	0	0.51	0.34
	(0.01)	(0.01)	(0.00)	(0.01)	(0.01)

(continued on next page)

Table B.3: (continued)

	High-High	High-Low	Low-High	Low-Low	Not sig.
South					
4th quintile	0.29	0.12	0	0.27	0.32
	(0.01)	(0.01)	(0.00)	(0.01)	(0.01)
5th quintile	0.6	0.15	0	0.04	0.2
	(0.01)	(0.01)	(0.00)	(0.00)	(0.01)
Midwest					
1st quintile	0.02	0.01	0	0.41	0.56
	(0.00)	(0.00)	(0.00)	(0.01)	(0.01)
2nd quintile	0.03	0.01	0	0.41	0.55
	(0.00)	(0.00)	(0.00)	(0.01)	(0.01)
3rd quintile	0.13	0.04	0	0.32	0.51
	(0.01)	(0.01)	(0.00)	(0.01)	(0.02)
4th quintile	0.44	0.08	0	0.1	0.37
	(0.02)	(0.01)	(0.00)	(0.01)	(0.02)
5th quintile	0.68	0.05	0	0.01	0.27
	(0.02)	(0.01)	(0.00)	(0.00)	(0.01)
West					
1st quintile	0.2	0.02	0	0.23	0.54
	(0.01)	(0.00)	(0.00)	(0.01)	(0.02)
2nd quintile	0.31	0.02	0.01	0.12	0.54
	(0.02)	(0.01)	(0.00)	(0.01)	(0.02)
3rd quintile	0.47	0.03	0.01	0.08	0.4
	(0.02)	(0.01)	(0.00)	(0.01)	(0.02)
4th quintile	0.76	0.04	0	0.04	0.16
	(0.02)	(0.01)	(0.00)	(0.01)	(0.01)
5th quintile	0.91	0.02	0	0	0.06
	(0.01)	(0.00)	(0.00)	(0.00)	(0.01)

(continued on next page)

Table B.3: (continued)

B. *Relative distance to social neighbours*					
	High-High	High-Low	Low-High	Low-Low	Not sig.
All regions					
1st quintile	0.15	0.08	0	0.38	0.38
	(0.01)	(0.00)	(0.00)	(0.01)	(0.01)
2nd quintile	0.23	0.05	0	0.32	0.4
	(0.01)	(0.00)	(0.00)	(0.01)	(0.01)
3rd quintile	0.33	0.05	0	0.26	0.37
	(0.01)	(0.00)	(0.00)	(0.01)	(0.01)
4th quintile	0.37	0.05	0	0.27	0.36
	(0.01)	(0.00)	(0.00)	(0.01)	(0.01)
5th quintile	0.64	0.02	0.01	0.1	0.24
	(0.01)	(0.00)	(0.00)	(0.01)	(0.01)
Northeast					
1st quintile	0.34	0.02	0	0.2	0.44
	(0.02)	(0.00)	(0.00)	(0.02)	(0.02)
2nd quintile	0.41	0.01	0	0.13	0.45
	(0.02)	(0.00)	(0.00)	(0.01)	(0.01)
3rd quintile	0.56	0	0	0.08	0.35
	(0.02)	(0.00)	(0.00)	(0.01)	(0.02)
4th quintile	0.76	0	0	0.04	0.2
	(0.01)	(0.00)	(0.00)	(0.01)	(0.01)
5th quintile	0.9	0	0.01	0.01	0.07
	(0.01)	(0.00)	(0.00)	(0.00)	(0.01)
South					
1st quintile	0.08	0.11	0	0.5	0.3
	(0.01)	(0.01)	(0.00)	(0.01)	(0.01)
2nd quintile	0.15	0.08	0	0.47	0.3
	(0.01)	(0.01)	(0.00)	(0.01)	(0.01)
3rd quintile	0.21	0.1	0	0.41	0.27
	(0.01)	(0.01)	(0.00)	(0.01)	(0.01)

(continued on next page)

Table B.3: (continued)

	High-High	High-Low	Low-High	Low-Low	Not sig.
South					
4th quintile	0.33	0.06	0	0.37	0.24
	(0.01)	(0.01)	(0.00)	(0.01)	(0.01)
5th quintile	0.43	0.04	0	0.2	0.33
	(0.01)	(0.01)	(0.00)	(0.01)	(0.01)
Midwest					
1st quintile	0.14	0.05	0	0.29	0.51
	(0.01)	(0.01)	(0.00)	(0.01)	(0.01)
2nd quintile	0.16	0.04	0	0.29	0.51
	(0.01)	(0.00)	(0.00)	(0.01)	(0.01)
3rd quintile	0.22	0.02	0	0.28	0.48
	(0.01)	(0.00)	(0.00)	(0.01)	(0.01)
4th quintile	0.16	0.02	0	0.24	0.58
	(0.01)	(0.00)	(0.00)	(0.01)	(0.01)
5th quintile	0.46	0.04	0	0.21	0.429
	(0.03)	(0.01)	(0.00)	(0.02)	(0.02)
West					
1rd quintile	0.51	0.07	0	0.13	0.29
	(0.03)	(0.01)	(0.00)	(0.02)	(0.03)
2th quintile	0.56	0.05	0	0.11	0.29
	(0.03)	(0.01)	(0.00)	(0.01)	(0.02)
3rd quintile	0.6	0.02	0	0.11	0.26
	(0.02)	(0.00)	(0.00)	(0.01)	(0.02)
4th quintile	0.6	0.01	0	0.09	0.29
	(0.02)	(0.00)	(0.84)	(0.01)	(0.02)
5th quintile	0.59	0.02	0.01	0.07	0.31
	(0.01)	(0.00)	(0.00)	(0.01)	(0.01)

Notes: Panels A and B each correspond to a multinomial logistic regression with cluster membership as the outcome. Fitted probabilities and standard errors (in brackets) are obtained using the approach of Fox and Andersen (2006). Local Moran index values measure autocorrelation in EB-standardised (Assunção and Reis, 1999) Democratic two-party vote shares as of the 2020 US presidential election, in the social space spanned by the social neighbours of each area: the 1,347 most connected areas as measured by the Social Connectedness Index (SCI) (Bailey et al., 2020).

References

Abrams, S. J. and M. P. Fiorina (2012). "The Big Sort" That Wasn't: A Skeptical Reexamination. *PS: Political Science & Politics 45*(2), 203–210.

Anselin, L. (1995). Local Indicators of Spatial Association—LISA. *Geographical Analysis 27*(2), 93–115.

Anselin, L. (1996). The Moran Scatterplot as an ESFA Tool to Assess Local Instability in Spatial Association. In M. Fischer, H. Scholten, and D. Unwin (Eds.), *Spatial Analytical Perspectives on GIS in Environmental and Socio-Economic Sciences*. London, UK: Taylor & Francis.

Assunção, R. M. and E. A. Reis (1999). A New Proposal to Adjust Moran's I for Population Density. *Statistics in Medicine 18*(16), 2147–2162.

Bailey, M., R. Cao, T. Kuchler, J. Stroebel, and A. Wong (2018). Social Connectedness: Measurement, Determinants, and Effects. *Journal of Economic Perspectives 32*(3), 259–80.

Bailey, M., P. Farrell, T. Kuchler, and J. Stroebel (2020). Social Connectedness in Urban Areas. *Journal of Urban Economics 118*, 103264.

Baybeck, B. and R. Huckfeldt (2002a). Spatially Dispersed Ties Among Interdependent Citizens: Connecting Individuals and Aggregates. *Political Analysis 10*(3), 261–275.

Baybeck, B. and R. Huckfeldt (2002b). Urban Contexts, Spatially Dispersed Networks, and the Diffusion of Political Information. *Political Geography 21*(2), 195–220.

Benjamini, Y. and Y. Hochberg (1995). Controlling the False Discovery Rate: A Practical and Powerful Approach to Multiple Testing. *Journal of the Royal Statistical Society: Series B (Methodological) 57*(1), 289–300.

Bishop, B. (2020). For Most Americans, the Local Presidential Vote Was a Landslide. *The Daily Yonder*.

Bishop, B. and R. G. Cushing (2009). *The Big Sort: Why the Clustering of Like-Minded America is Tearing Us Apart*. New York, NY: Houghton Mifflin Harcourt.

Bivand, R. (2022). R Packages for Analyzing Spatial Data: A Comparative Case Study with Areal Data. *Geographical Analysis 54*(3), 488–518.

Boxell, L., M. Gentzkow, and J. M. Shapiro (2017). Greater Internet Use Is Not Associated with Faster Growth in Political Polarization Among US Demographic Groups. *Proceedings of the National Academy of Sciences 114*(40), 10612–10617.

Brown, J. R., E. Cantoni, R. D. Enos, V. Pons, and E. Sartre (2023). The Increase in Partisan Segregation in the United States. Nottingham Interdisciplinary Centre for Economic and Political Research (NICEP) Discussion Paper 2023-09.

Brown, J. R. and R. D. Enos (2021). The Measurement of Partisan Sorting for 180 Million Voters. *Nature Human Behaviour 5*(8), 998–1008.

Charoenwong, B., A. Kwan, and V. Pursiainen (2020). Social Connections with COVID-19–Affected Areas Increase Compliance with Mobility Restrictions. *Science Advances 6*(47), eabc3054.

Chen, J. and J. Rodden (2013). Unintentional Gerrymandering: Political Geography and Electoral Bias in Legislatures. *Quarterly Journal of Political Science 8*(3), 239–269.

Darmofal, D. and R. Strickler (2019). *Demography, Politics, and Partisan Polarization in the United States, 1828-2016*. Cham, CH: Springer Nature.

de Castro, M. C. and B. H. Singer (2006). Controlling the False Discovery Rate: A New Application to Account for Multiple and Dependent Tests in Local Statistics of Spatial Association. *Geographical Analysis 38*(2), 180–208.

Duggan, M., N. B. Ellison, C. Lampe, A. Lenhart, and M. Madden (2015). Demographics of Key Social Networking Platforms. Pew Research Center.

Efron, B. and T. Hastie (2016). *Computer Age Statistical Inference: Algorithms, Evidence, and Data Science*. Cambridge, UK: Cambridge University Press.

Enos, R. D. (2017). *The Space Between Us: Social Geography and Politics*. New York, NY: Cambridge University Press.

Ethington, P. J. and J. A. McDaniel (2007). Political Places and Institutional Spaces: The Intersection of Political Science and Political Geography. *Annual Review of Political Science 10*(1), 127–142.

Finkel, E. J., C. A. Bail, M. Cikara, P. H. Ditto, S. Iyengar, S. Klar, L. Mason, M. C. McGrath, B. Nyhan, D. G. Rand, L. J. Skitka, J. A. Tucker, J. J. V. Bavel, C. S. Wang, and J. N. Druckman (2020). Political Sectarianism in America. *Science 370*(6516), 533–536.

Fischer, C. S. (1982). *To Dwell Among Friends: Personal Networks in Town and City*. Chicago, IL: University of Chicago Press.

Fowler, C. S., N. Frey, D. C. Folch, N. Nagle, and S. Spielman (2020). Who are the People in my Neighborhood?: The "Contextual Fallacy" of Measuring Individual Context with Census Geographies. *Geographical Analysis 52*(2), 155–168.

Fox, J. and R. Andersen (2006). Effect Displays for Multinomial and Proportional-Odds Logit Models. *Sociological Methodology 36*(1), 225–255.

Fox, J. and S. Weisberg (2019). *An R Companion to Applied Regression* (3rd ed.). Thousand Oaks CA: SAGE Publications Inc.

Gentzkow, M. (2016). Polarization in 2016. White Paper, Toulouse Network for Information Technology.

Geverdt, D. (2018). Education Demographic and Geographic Estimates Program (EDGE): Locale Boundaries File Documentation, 2017 (NCES 2018-115). Department of Education. Washington, DC: National Center for Education Statistics.

Geverdt, D. (2019). Education Demographic and Geographic Estimates Program (EDGE): ZIP Code Tabulation Area (ZCTA) Locale Assignments File Documentation (NCES2018-077). Department of Education. Washington, DC: National Center for Education Statistics.

Gimpel, J. G. and I. S. Hui (2015). Seeking Politically Compatible Neighbors? The Role of Neighborhood Partisan Composition in Residential Sorting. *Political Geography 48*, 130–142.

Gimpel, J. G. and A. Reeves (2022). Electoral Geography, Political Behavior and Public Opinion. In T. J. Rudolph (Ed.), *Handbook on Politics and Public Opinion*. Northampton, MA: Edward Elgar Publishing.

Granovetter, M. (1983). The strength of weak ties: A network theory revisited. *Sociological theory*, 201–233.

Granovetter, M. S. (1973). The Strength of Weak Ties. *American Journal of Sociology 78*(6), 1360–1380.

Holtz, D., M. Zhao, S. G. Benzell, C. Y. Cao, M. A. Rahimian, J. Yang, J. Allen, A. Collis, A. Moehring, T. Sowrirajan, D. Ghosh, Y. Zhang, P. S. Dhillon, C. Nicolaides, D. Eckles, and S. Aral (2020). Interdependence and the Cost of

Uncoordinated Responses to COVID-19. *Proceedings of the National Academy of Sciences 117*(33), 19837–19843.

Hopkins, D. (2017). *Red Fighting Blue: How Geography and Electoral Rules Polarize American Politics*. New York, NY: Cambridge University Press.

Huckfeldt, R. R. (1982). *Politics in Context: Assimilation and Conflict in Urban Neighborhoods*. New York, NY: Agathon Press.

Huckfeldt, R. R. (1983). Social Contexts, Social Networks, and Urban Neighborhoods: Environmental Constraints on Friendship Choice. *American Journal of Sociology 89*(3), 651–669.

Huckfeldt, R. R. and J. Sprague (1995). *Citizens, Politics, and Social Communication: Information and Influence in an Election Campaign*. New York, NY: Cambridge University Press.

Iyengar, S., Y. Lelkes, M. Levendusky, N. Malhotra, and S. J. Westwood (2019). The Origins and Consequences of Affective Polarization in the United States. *Annual Review of Political Science 22*(1), 129–146.

Iyengar, S. and S. J. Westwood (2015). Fear and Loathing across Party Lines: New Evidence on Group Polarization. *American Journal of Political Science 59*(3), 690–707.

Johnston, R., D. Manley, K. Jones, and R. Rohla (2020). The Geographical Polarization of the American Electorate: A Country of Increasing Electoral Landslides? *GeoJournal 85*(1), 187–204.

Johnston, R. and C. Pattie (2014). Social Networks, Geography and Neighbourhood Effects. In *The SAGE Handbook of Social Network Analysis*, London, UK. SAGE Publications Ltd.

Kinsella, C., C. McTague, and K. Raleigh (2021). Closely and Deeply Divided: Purple Counties in the 2016 Presidential Election. *Applied Geography 127*, 102386.

Kinsella, C., C. McTague, and K. N. Raleigh (2015). Unmasking Geographic Polarization and Clustering: A Micro-Scalar Analysis of Partisan Voting Behavior. *Applied Geography 62*, 404–419.

Kuchler, T., D. Russel, and J. Stroebel (2022). JUE Insight: The Geographic Spread of COVID-19 Correlates with the Structure of Social Networks as Measured by Facebook. *Journal of Urban Economics 127*, 103314.

Kwan, M.-P. (2012). The Uncertain Geographic Context Problem. *Annals of the Association of American Geographers 102*(5), 958–968.

Li, X. and L. Anselin (2023). *rgeoda: R Library for Spatial Data Analysis*. R package version 0.0.1.

Logan, J. R. and G. D. Spitze (1994). Family Neighbors. *American Journal of Sociology 100*(2), 453–476.

Makridis, C. A. (2022). The Social Transmission of Economic Sentiment on Consumption. *European Economic Review 148*, 104232.

Martin, G. J. and S. W. Webster (2020). Does Residential Sorting Explain Geographic Polarization? *Political Science Research and Methods 8*(2), 215–231.

Mason, L. (2015). "I Disrespectfully Agree": The Differential Effects of Partisan Sorting on Social and Issue Polarization. *American Journal of Political Science 59*(1), 128–145.

McGhee, E. (2020). Partisan Gerrymandering and Political Science. *Annual Review of Political Science 23*(1), 171–185.

McPherson, M., L. Smith-Lovin, and J. M. Cook (2001). Birds of a Feather: Homophily in Social Networks. *Annual Review of Sociology 27*(1), 415–444.

Mettler, S. and T. Brown (2022). The Growing Rural-Urban Political Divide and Democratic Vulnerability. *The ANNALS of the American Academy of Political and Social Science 699*(1), 130–142.

Mok, D., R. Basu, and B. Wellman (2007). Did Distance Matter Before the Internet?: Interpersonal Contact and Support in the 1970s. *Social Networks 29*(3), 430–461.

Mok, D., B. Wellman, and J. Carrasco (2010). Does Distance Matter in the Age of the Internet? *Urban Studies 47*(13), 2747–2783.

Mummolo, J. and C. Nall (2017). Why Partisans Do Not Sort: The Constraints on Political Segregation. *The Journal of Politics 79*(1), 45–59.

Mutz, D. C. (2002). Cross-Cutting Social Networks: Testing Democratic Theory in Practice. *The American Political Science Review 96*(1), 111–126.

Myers, A. S. (2013). Secular Geographical Polarization in the American South: The Case of Texas, 1996–2010. *Electoral Studies 32*(1), 48–62.

Nall, C. (2018). *The Road to Inequality: How the Federal Highway Program Polarized America and Undermined Cities*. New York, NY: Cambridge University Press.

Pettigrew, T. F. and L. R. Tropp (2006). A Meta-Analytic Test of Intergroup Contact Theory. *Journal of Personality and Social Psychology 90*(5), 751.

Rodden, J. (2015). *Geography and Gridlock in the United States*, pp. 104–120. Cambridge University Press.

Rodden, J. (2019). *Why Cities Lose: The Deep Roots of the Urban-Rural Political Divide*. New York, NY: Cambridge University Press.

Rohla, R., R. Johnston, K. Jones, and D. Manley (2018). Spatial Scale and the Geographical Polarization of the American Electorate. *Political Geography 65*, 117–122.

Scala, D. J. and K. M. Johnson (2017). Political Polarization Along the Rural-Urban Continuum? The Geography of the Presidential Vote, 2000–2016. *The ANNALS of the American Academy of Political and Social Science 672*(1), 162–184.

Takhteyev, Y., A. Gruzd, and B. Wellman (2012). Geography of Twitter Networks. *Social Networks 34*(1), 73–81.

Vogels, E. A. and M. Anderson (2021). Social Media Use in 2021. Pew Research Center.

Vogels, E. A., B. Auxier, and M. Anderson (2021). Partisan Differences in Social Media Use Show Up for Some Platforms, but Not Facebook. Pew Research Center.

Voting and Election Science Team (2020). *2020 Precinct-Level Election Results*. Harvard Dataverse. Dataset version 40.

Walker, K. and M. Herman (2023). *tidycensus: Load US Census Boundary and Attribute Data as 'tidyverse' and 'sf'-Ready Data Frames*. R package version 1.4.3.

Walker, K. and B. Rudis (2023). *tigris: Load Census TIGER/Line Shapefules*. R package version 2.0.1.

Wellman, B. (1979). The Community Question: The Intimate Networks of East Yorkers. *American Journal of Sociology 84*(5), 1201–1231.

Wellman, B. (1996). Are Personal Communities Local? A Dumptarian Reconsideration. *Social Networks 18*(4), 347–354.

Wellman, B. and S. Potter (1999). *Networks in the Global Village*. New York, NY: Routledge.

Wellman, B., A. Quan-Haase, J. Boase, W. Chen, K. Hampton, I. Díaz, and K. Miyata (2003). The Social Affordances of the Internet for Networked Individualism. *Journal of Computer-Mediated Communication 8*(3), JCMC834.

Wilson, R. (2022). The Impact of Social Networks on EITC Claiming Behavior. *The Review of Economics and Statistics 104*(5), 929–945.

Zhao, M., D. Holtz, and S. Aral (2021). Interdependent Program Evaluation: Geographic and Social Spillovers in COVID-19 Closures and Reopenings in the United States. *Science Advances 7*(31), eabe7733.